JMEPEG (2006) 15:155-160
DOI: 10.1361/105994906X95805

1059-9495/$19.00

Femtosecond Laser Micromachining of Aluminum Surfaces Under Controlled Gas Atmospheres

G.M. Robinson and M.J. Jackson

(Submitted November 4, 2005; in revised form December 19, 2005)

The interaction of 180 femtosecond (fs), 775 nm laser pulses with the surface of aluminum under controlled gas atmospheres at ambient pressure has been investigated to study material redeposition, residual surface roughness, and ablation rate. The effect of using various gases to protect the surface of the material appears to interfere with the effects of the plasma and can change the resulting microstructure of the machined surface. By varying the combinations of fluence and laser-scanning speed during ultrafast ablation at high repetition rates, an optimum micromachining condition can be reached, depending on the type of gas used during machining. The debris produced under certain laser-machining conditions tends to produce pure aluminum nanoparticles that are deposited very close to the machined feature by the gas used to protect the surface of the aluminum.

Keywords ablation, aluminum, nanoparticles, surface engineering, ultrafast lasers

1. Introduction

When a laser beam is focused on the area to be machined, the fluence, or energy per unit area, is high enough to ablate the material when using the appropriate laser. A problem with laser micromachining is the generation of a recast layer of deposited material (Ref 1). A recast layer is ablated material that has prematurely cooled (Ref 2). It either condenses around the ablation zone, forming a wall of material, or condenses in droplet form on the surface of the workpiece. The surrounding protective gas is responsible for ejecting the ablated material under certain conditions (Ref 3, 4). Therefore, the affect of different assist gases on the surface of the substrate has been investigated. Various assist gases used in the present work are air, oxygen, helium, and argon. Small cubic trenches were machined from the surface, and it was found that the structure of the surface was dramatically affected by a combination of fluence, type of gas used, and scan speed.

2. Laser Material Interactions

The principle of laser material removal is that laser light is focused on the material surface where energy is absorbed. This energy is converted to heat. The maximum depth where absorption occurs is called the *penetration depth* and leads to the conduction of heat into the material. The energy absorbed for a CO_2 laser is about 20%, the energy absorbed for an Nd:YAG laser or a femtosecond (fs) laser is approximately 40 to 80%, and the rest of the energy is reflected. Special care must be taken with optics, and special antireflective coatings must be applied to prevent beams penetrating into unwanted areas of the system. Laser energy is converted to heat only as far as the penetration depth. At the penetration depth, the power density is approximately 1/*e* of the original density at the surface; for a CO_2 laser this is about 15 nm, and for an Nd:YAG laser this is about 5 nm. The conduction of heat into the bulk depends on the timescale of the pulses.

The mechanism that lasers use to remove material is called *ablation*. Ablation is achieved by melting and vaporizing the material, which is then ejected from the vicinity of the surface and is governed by power density. However, the ejected material can be deposited near to the melt region where it freezes and is known as the *recast layer* (Fig. 1).

For a power density of 10^{-9} W/cm^2 the melting point is reached in 300 ns; if the power density is increased tenfold, this time is reduced tenfold to 30 ns.

The high vaporization rate then causes a shock wave that can reach speeds of 3 km/s. The expulsion of material occurs due to the high pressure created in the melt and the explosive-

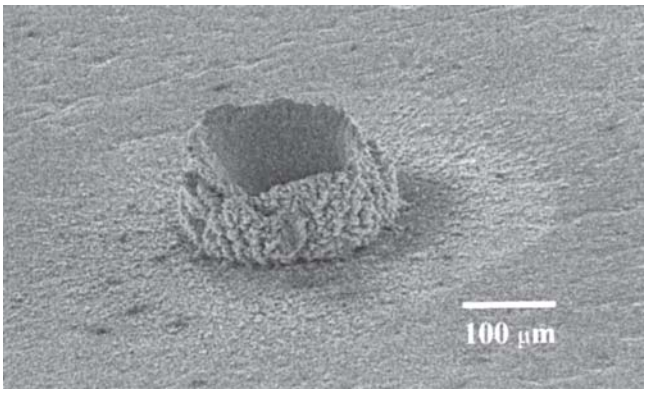

Fig. 1 Recast layer created close to the melt region

This paper was presented at the fourth International Surface Engineering Congress and Exposition held August 1-3, 2005 in St. Paul, MN.

G.M. Robinson and **M.J. Jackson,** Birck Nanotechnology Centre, Purdue University, West Lafayette, IN 47907-2021. Contact e-mail: jacksomj@purdue.edu.

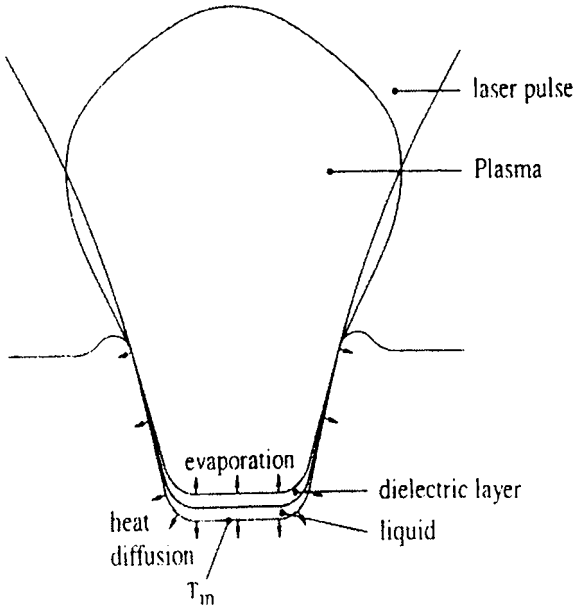

Fig. 2 Relationship between plasma generated during the laser pulse interaction with the workpiece material and its surroundings (Ref 5)

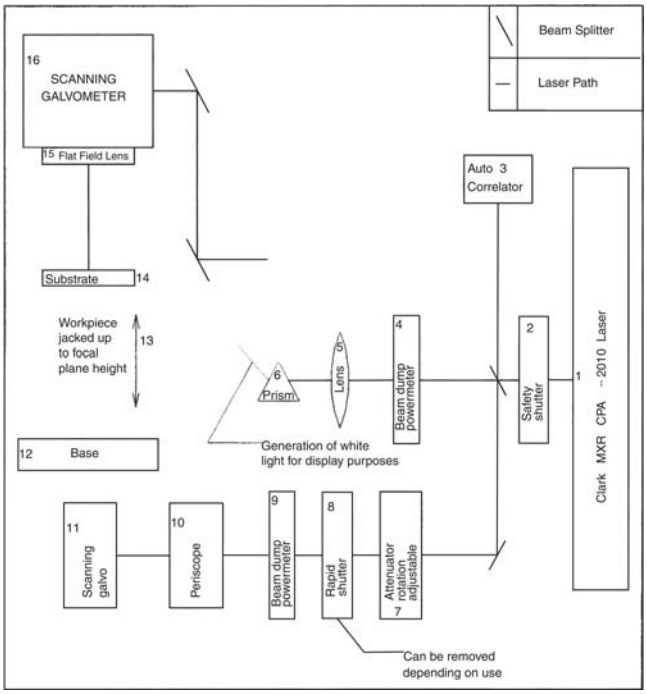

Fig. 3 Schematic diagram of the apparatus used during fs laser micromachining experiments

like boiling of the superheated liquid after the end of the laser pulse. This ejected material can reform. Sometimes it is not always totally vaporized, especially if it is from a deep trench that may cool quickly and reform.

Nanosecond lasers produce heat flow, whereas fs lasers do not because no melt pool has been produced. Femtosecond laser pulses machine with minimal heat generation, where the heat-affected zone (HAZ) is given by the equation HAZ ~ $(D \cdot t)^{1/2}$, where D is the thermal diffusion coefficient and t is the pulse duration.

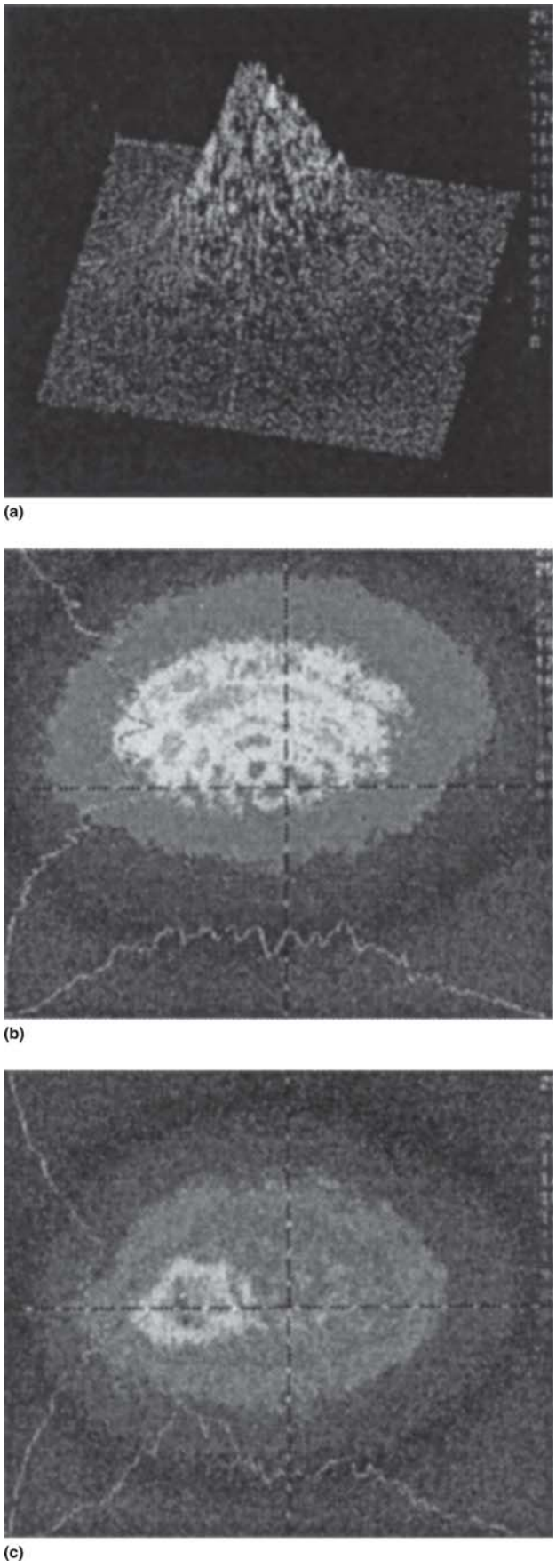

Fig. 4 Three-dimensional image of a beam showing (a) mode, (b) diffraction effects, and (c) off-center thermal profile

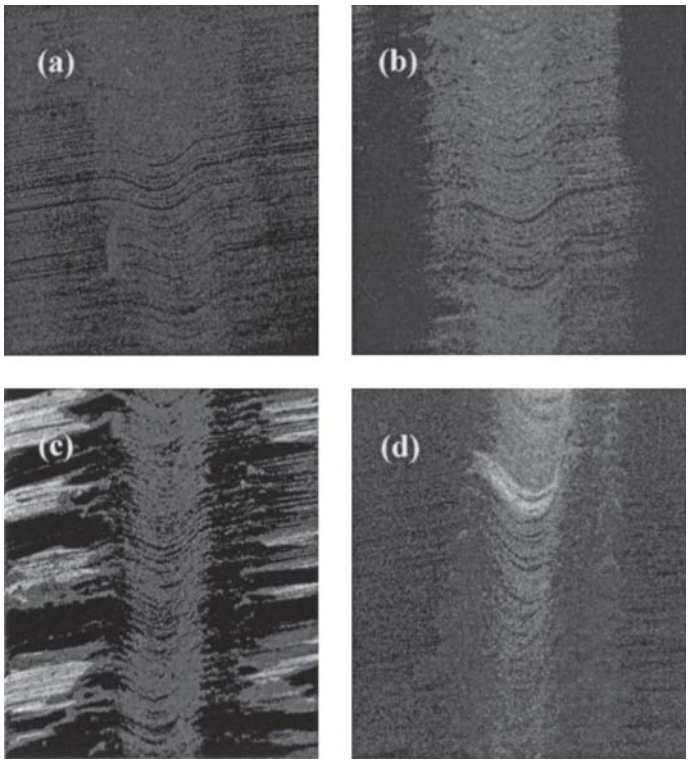

Fig. 5 Effects of using different assist gases on the surface of aluminum. The track width is ~100 μm: (a) helium; (b) argon; (c) air; and (d) nitrogen

Heat flow produces the melt pool, around which the bulk of the material heats up. If rapid heating occurs, then the damage to the material is incurred at a greater depth than is desired, which is the HAZ. Clearly, the relationship HAZ ~ $(D \cdot t)^{1/2}$ states that shorter pulse durations will decrease the amount of HAZ. The diffusion length for a 20 ns laser is 365 times longer than that for a 150 fs laser. The nanosecond diffusion length is 1×10^{-4} m, and the approximate diffusion length for metals is 1×10^{-6} m. The fs diffusion length is approximately 4×10^{-7} m, where 1 fs is equal to 10^{-15} tenths of a second. Materials react to induced heat pulses in picoseconds (i.e., 10^{-12} tenths of a second). Therefore, the material can be heated and removed before the surrounding material can react, hence there can be no heat flow in the fs case.

Material at the top of the surface is removed by evaporation, and at the sidewalls of the hole or trench the material is forced away by the plasma. Both effects cause the redeposition of material elsewhere.

Plasma pressure is exerted on the liquid. At the end of the pulse, the pressure suddenly drops and causes boiling of the superheated liquid to occur.

Ablation occurs at the end of the pulse, and it has been discovered that for a given fluence there is a maximum ablation depth for a given pulse length. Material removal rates can be difficult to calculate due to the redeposition of the molten material.

The ablation of metals is caused by the absorption of laser energy, which is a three-step process: (1) absorption of the photon by electrons (10^{-15} s); (2) energy transferred to the lattice (10^{-12} s); and (3) heat transferred to the lattice (10^{-12} s).

Ablation at the end of the pulse is due to the relatively thick superheated layer, which continues to evaporate as long as the surface is above the boiling temperature (Fig. 2).

Redeposition may occur in the path of a track, which has yet to be machined. In this case, more material has to be removed. Deposition may occur elsewhere in a noncritical area. This is what makes calculating material removal rates difficult. In the case of fs pulses during the solid-to-liquid transformation, there is no melting because it happens so quickly that it is considered instantaneous. Due to this effect, there is no heat transfer, and there is a debate as to whether the HAZ exists or not.

2.1 Ti:Sapphire Lasers

Ti:Sapphire lasers produce pulses in the fs time regime. Short, low-power nanojoule fs pulses are created by an erbium-doped fiber laser. The amplification of these low-power pulses is required to produce a useful power output, but there are problems associated with this. These problems are overcome by using chirped pulse amplification (CPA). The pulse is stretched, amplified, and then compressed to create a high-intensity fs pulse.

The problem with directly amplifying short pulses is their tendency to stretch in time; the pulse may be amplified but it will no longer be on the fs timescale. Femtosecond pulses also tend to destroy the medium through which they travel.

The CPA avoids these problems by the basic principle of stretching short pulses to reduce the peak intensity. The pulse is then compressed back to the original timescale. The fs pulse is made up of several wavelengths. The diffraction gratings or chirping mirrors separate out the different wavelengths of the pulse. This is done because the grating causes the individual frequencies to reflect at different angles. Thus, light from the

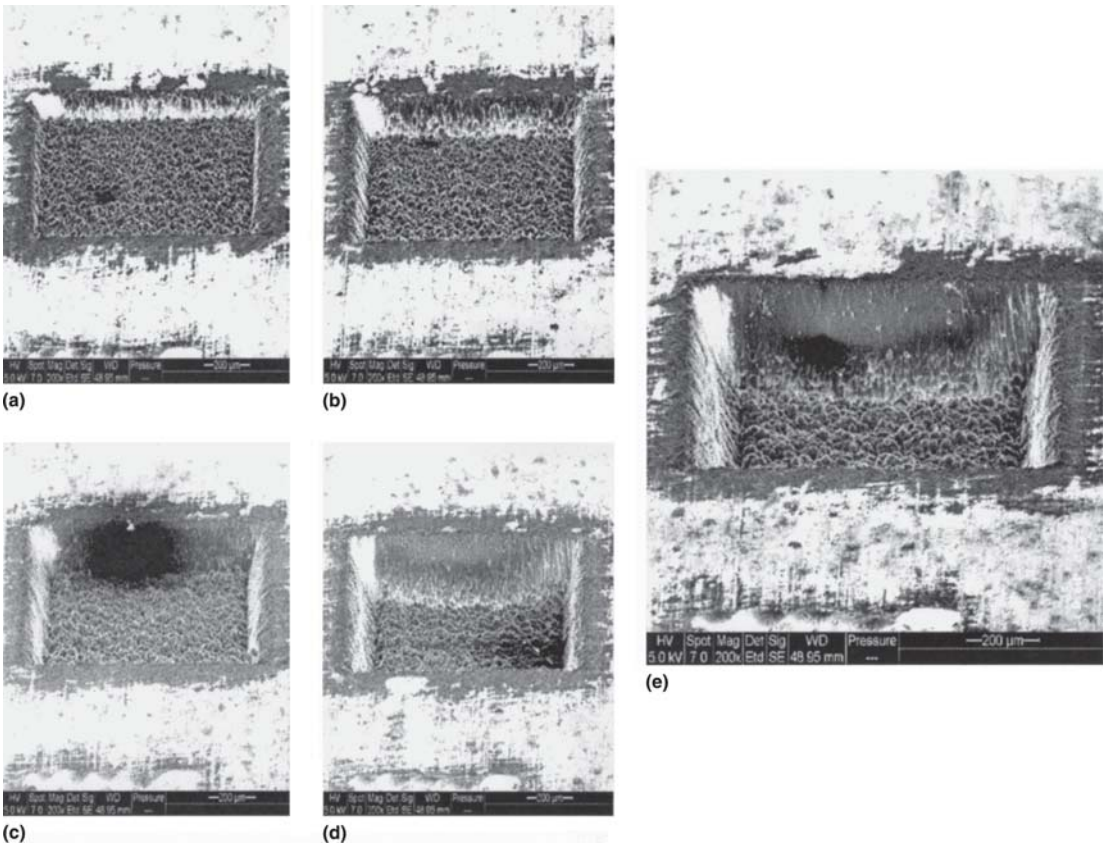

Fig. 6 Trench structure variation at 1 mm/s and a varying number of overscans: (a) 1 overscan; (b) 2 overscans; (c) 3 overscans; (d) 4 overscans; and (e) 5 overscans

same pulse travels different distances, which tends to stretch the pulse and reduce the peak intensity.

The stretched pulses are let into the regenerative cavity for amplification. The pulse is sent along a certain path. At a point in this path, it passes through a Ti:Sapphire crystal, which is the gain medium. This is pumped by an Nd:YAG laser. Each time the stretched pulse passes through the cavity it gains a little more energy, receiving a boost from the interactions in the cavity.

Along a part of this path, there is a component that reflects the pulse if it is not of high enough energy. It is then sent back into the regenerative amplifier to gain more energy until it reaches some critical value. When this value is reached, the pulse encounters the device and then has enough energy to escape from it.

Thus, the pulses have been amplified in terms of power but are stretched in terms of time. An exact reversal of the process that stretched the pulse is then applied to recapture the original pulse length. The pulses are now at full power and are on the fs timescale. The pockel cell and polarizer perform the tasks of timing the entry of pulses into the regenerative amplifier, and determining how the pulses are let out of the cavity and how the gain is received.

3. Experimental Apparatus

The experimental apparatus consisted of a Clark MXR (Dexter, MI) chirped pulse laser and a scanning galvanometer, so that the pulsed beam of light is directed to the surface of the aluminum workpiece. The laser system was set up as shown in Fig. 3.

To characterize the effects of micromachining, it is important to know the characteristics of the beam. Figure 2 shows the mode of the laser, which is identified as TEM_{00}, and also where the concentrations of optical energy and temperature are located. The laser power and beam profile were assessed using a Spyricon (Logan, UT) beam profilometer (Fig. 4).

4. Experimental Results and Discussion

4.1 Effects of Gas Environment

Figure 5 shows the result of machining a single trench under different gases. In each case the spot size, fluence, and scan speed are constant. It can be seen for air, nitrogen, and argon there are significant recast layer deposits. Improvement is shown when the assist gas used is helium, where there is a significant reduction in the size and amount of debris particles on the surface of the aluminum.

4.2 Effects of Machining

The following results were conducted in an ambient airflow generated at 150 μJ/pulse: the spot diameter is approximately 30 μm and is slightly elliptical. The overlap between lines is 10 μm. The results in Fig. 6 show the effect of increasing the number of overscans in aluminum while maintaining the laser power and scan speed. The textured surface produced at the base of the cube increases in variability with an increasing number of scans. It can be seen that the relief of the sidewalls

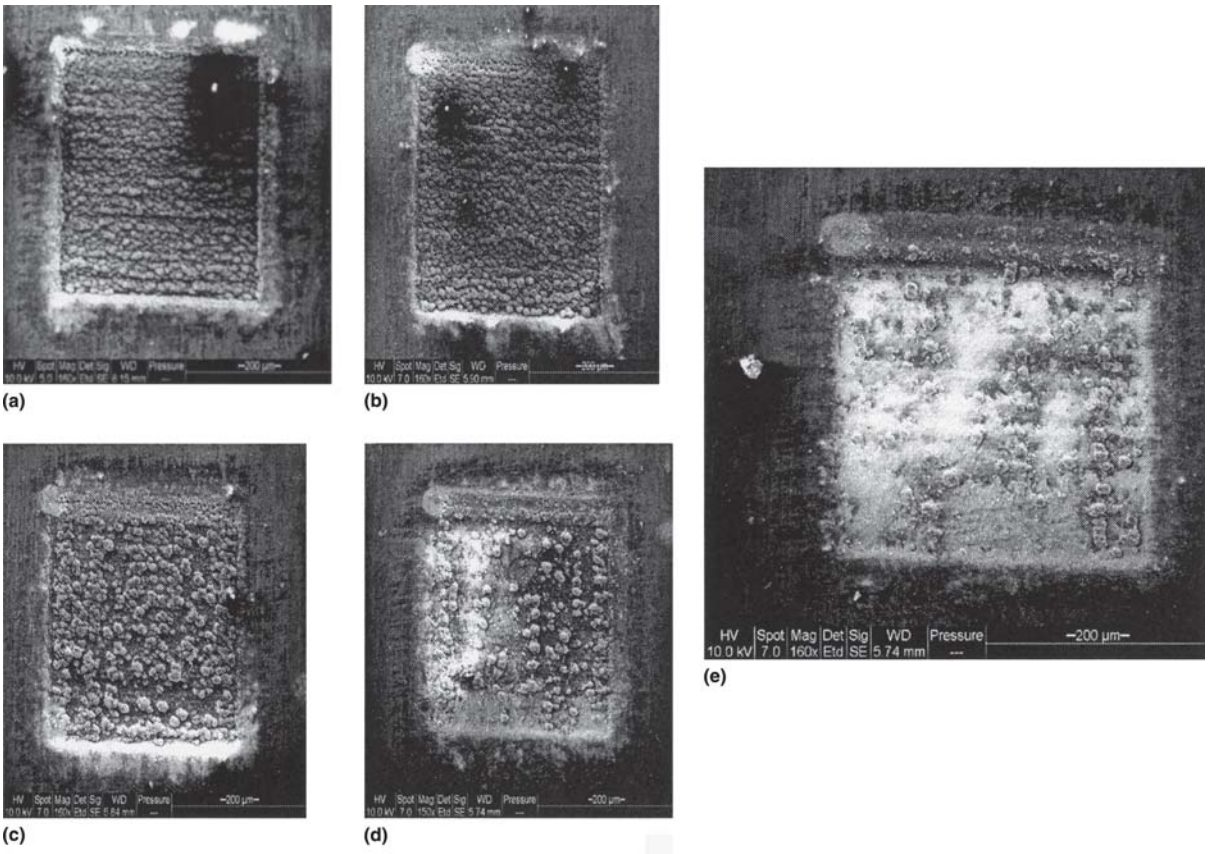

Fig. 7 Trench structure variation at 21 overscans and with increasing scan speeds: (a) 1 mm/s; (b) 2 mm/s; (c) 3 mm/s; (d) 4 mm/s; and (e) 5 mm/s

becomes more severe as the number of overscans increases. This may be attributed to the nature and shape of the Gaussian profile of the beam.

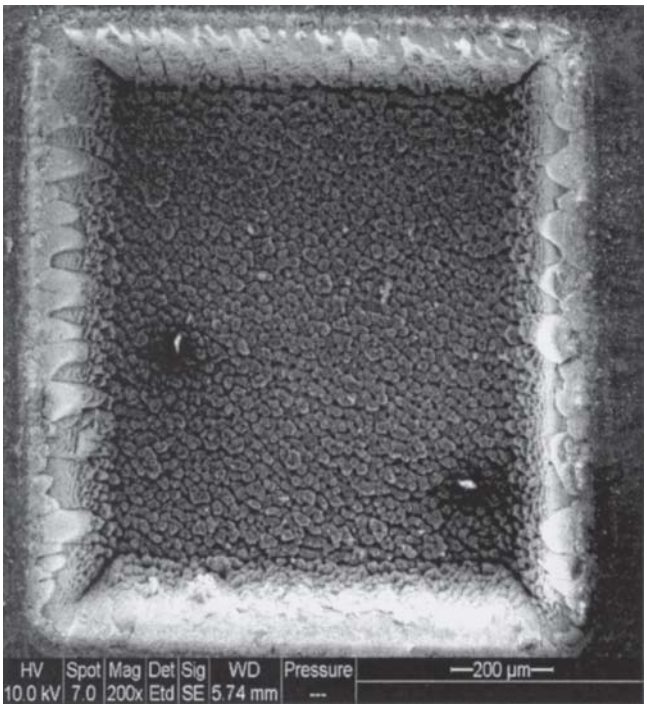

Fig. 8 Effects of fast scan speed (10 mm/s) and 50 overscans

The textured surface appears to be globules of metal that are left behind by the ablation of the surrounding matrix. Alternatively, the structured surface could be condensed droplets of recast material that have fallen and solidified. Alternatively, the texture could be locally solidified melt pools created by the heat from the plasma (heat from the beam directly evaporates material, therefore, if present, secondary heating effects are likely to arise from the plasma). Figure 7 shows that increasing the scan speed reduces the severity of surface texturing; however, the depth of the machined surface is severely reduced.

It could be reasoned that the best quality machined surface is machined with a combination of a fast scan speed to reduce texturing and many overscans to achieve a reasonable depth. This was examined and is shown in Fig. 8, where a scan speed of 10 mm/s was used to scan the surface 50 times. However, even with these parameters there is still significant texturing on the base (Fig. 8). Further experiments are required to conduct these experiments at varying power levels, where it could be reasoned that at very low power levels the formation of texture is reduced. The inherent problem with laser micromachining is the shape and nature of the Gaussian beam profile. This problem is manifest in trenches where the walls of the machined slot are not parallel.

5. Conclusions

This article has shown that micromachining is possible with fs lasers when combined with fast scanning speeds and large numbers of overscans. The effect of a shielding or assist gas is

also significant on the formation of recast layers. In comparison with other micromachining processes, further development work is required to ensure that laser micromachining is economically feasible.

References

1. M.J. Jackson, M.D.H. Gill, A.H. Khan, and W. O'Neill, Evaluation of Supersonic Nozzle Designs for Laser Micro Machining of High Speed Steels, Transactions of S.M.E, *J. Manufact. Proc.,* 2002, **4,** p 42-51
2. M.J. Jackson, G.M. Robinson, B. Mills, and W. O'Neill, Laser Micro Machining of Chromium Rich Die Steel Under Controlled Atmospheres: Proceedings of the Institution of Mechanical Engineers (London), *J. Eng. Manufact. B,* 2003, **217,** p 553-562
3. M.J. Jackson, G.M. Robinson, A.H. Khan, M.D.H. Gill, B. Mills, and W. O'Neill, Micromachining of High Chromium Content Steel Under Controlled Gas Atmospheres, Transactions of S.M.E., *J. Manufact. Proc.,* 2003, **5,** p 106-117
4. M.J. Jackson, G.M. Robinson, M.D.H. Gill, and W. O'Neill, The Effect of Nozzle Design on Laser Micro Machining of M2 Tool Steels, *J. Mater. Process. Technol.,* 2005, **160,** p 198-212
5. J.A. McGeough, Ed., *Micromachining of Engineering Materials*, Marcel Dekker, London, U.K., 2002